oretical results for the average number of nearest neighbors.[21]

Figure 10 shows the distributions for the hydrogen bond angles, θ and ϕ, illustrated in II. The potential functions prefer θ and

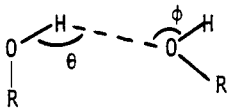

ϕ values of roughly 180 and 110° for the linear dimer in the gas phase at 0 K. The MHL results for the distributions are virtually identical with the TIP curves and reveal a broad variety of angular combinations for hydrogen bonds. As discovered previously for the other hydrogen bonded liquids,[3-7] the average hydrogen bond is bent about 20° in liquid methanol.

It is important to emphasize that in the liquids there is a continuous spectrum of hydrogen bond strengths and geometries as illustrated in Figures 8 and 10. The *average* hydrogen bond energy in liquid methanol is predicted here to be ca. 4.5 kcal/mol which translates to an enthalpy of ca. 3.3 kcal/mol.[6] Experimental measurements at ambient temperature refer to these average values and are not directly related to the results of quantum mechanical calculations for the absolute minimum on the potential surface for the dimer at 0 K. Thus, apparent discrepancies of 1-2 kcal/mol between theoretical and experimental results may be accounted for in this manner.[6,20]

IV. Conclusion

A number of important findings have emerged in this study. The similarity of the MHL and TIP results and their accord with the available experimental thermodynamic and structural data for liquid methanol are strong support for the viability of the TIP model. The results also indicate that it is unnecessary to explicitly include the methyl hydrogens to obtain a reasonable description of the liquid. In addition, this work establishes that sampling in Monte Carlo calculations can include internal rotations; however, further study is needed to define the limits of the procedure. The liquid's structure was not found to affect the distribution of dihedral angles for rotation of the methyl group in the methanol monomers. The previous description of the qualitative features of the structure of liquid methanol was confirmed.[6] The liquid primarily consists of hydrogen-bonded chains of various lengths. Most monomers are in one or two hydrogen bonds, however, some monomers participate in three hydrogen bonds corresponding to branch points in the chains. The hydrogen bonds are flexible and have smooth distributions of strengths and distortions.

Acknowledgment. Gratitude is expressed to the National Science Foundation (Grant CHE-7819446) for financial assistance. Acknowledgement is made to the donors of the Petroleum Research Fund, administered by the American Chemical Society, for support of this work. The work was also conducted with the aid of the National Resource for Computation in Chemistry under a grant from the National Science Foundation (Grant CHE-7721305) and the Basic Energy Science Division of the U.S. Department of Energy (Contract No. W-7405-ENG-48). Discussions with Professor W. A. P. Luck were most enlightening.

(20) Dill, J. D.; Allen, L. C.; Topp, W. C.; Pople, J. A. *J. Am. Chem. Soc.* **1975**, *97*, 7220.

(21) **Note Added in Proof**: In the review by Franks and Ives,[22] the authors state that the polymeric chains in liquid alcohols do not "exceed a complexity, *n*, of 5-7 molecules". However, in going over the original literature,[23] it appears that this claim was based on data for dilute solutions and not the pure liquids.

(22) Franks, F.; Ives, D. J. G. *Q. Rev., Chem. Soc.* **1966**, *20*, 1.

(23) Prigogine, I.; Defay, R. "Chemical Thermodynamics"; Longmans Green and Co.: London, 1954; Chapter 26 and references therein.

Simulation of Liquid Ethanol Including Internal Rotation[1]

William L. Jorgensen[2]

Contribution from the Department of Chemistry, Purdue University, West Lafayette, Indiana 47907. *Received May 20, 1980*

Abstract: A Monte Carlo statistical mechanics simulation of liquid ethanol at 25 °C has been performed by using the TIP model to describe the intermolecular interactions. Detailed structural and thermodynamic information has been obtained and compares favorably with experimental results including X-ray and infrared data. The internal rotation about the CO bond in the monomers was included in the calculations. The liquid's structure was not found to alter significantly the distribution for the dihedral angle from the ideal gas result. Winding hydrogen-bonded chains are ubiquitous in the liquid, and some branching of the chains is evident. Smaller oligomers are also present, though the occurrence of cyclic multimers is relatively uncommon. The monomers in the liquid experience an energetic continuum of environments covering a 20-kcal/mol range. Furthermore, the hydrogen bonds are distributed in both energy and geometry with the average hydrogen bond bent 15-20° from linear. The overall success of the simulation emphasizes the value and utility of the TIP based approach to modeling fluids.

I. Introduction

Interest in ethanol has been fluorishing due to its potential as a major fuel and raw material for the chemical industry.[3] Ethanol's importance as an organic solvent also makes it a key target for our theroetical studies of organic chemistry in solution. Progress cannot be made unless fluids with complex polar and nonpolar interactions can be treated. Consequently, a Monte Carlo statistical mechanics simulation of liquid ethanol at 25 °C has been carried out. This was facilitated by the recent development of transferable intermolecular potential functions (TIPS) for water, alcohols, and ethers.[4] The calculated structural and thermody-

(1) Quantum and Statistical Mechanical Studies of Liquids. 12.

(2) Camille and Henry Dreyfus Foundation Teacher-Scholar, 1978-1983; Alfred P. Sloan Foundation Fellow, 1979-1981.

(3) Anderson, E. *Chem. Eng. News* **1979**, *57* (*32*), 15.

(4) Jorgensen, W. L., penultimate preceding paper in this issue.

0002-7863/81/1503-345$01.00/0

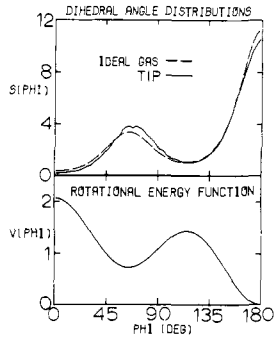

Figure 1. Bottom: potential energy (kcal/mol) for the internal rotation about the CO bond in ethanol. The trans and gauche minima occur at ϕ = 180 and 64°, respectively. Top: population distributions for the dihedral angle ϕ from a Boltzmann distribution for the ideal gas and from the TIP-based Monte Carlo simulation of liquid ethanol. The units for $S(\phi)$ are mole fraction per degree × 10^{-3}.

namic results for ethanol reported here compare well with the available experimental data. This is a major success for the TIP model and a most promising sign for treating even more complex organic liquids and solutions.

A particularly novel aspect of the simulation is that the internal rotation about the CO bond in the ethanol monomers has been included. The liquid's structure is not found to affect significantly the distribution for the dihedral angle or the trans to gauche ratio from the ideal gas expectations. Like methanol, liquid ethanol consists primarily of winding hydrogen-bonded chains.[5]

II. Computational Procedure

A. The Potential Function and Rotational Barrier. The TIP function for ethanol was used to describe the intermolecular interactions between monomers in the liquid. It has been discussed in detail previously.[4] Summarizing, an ethanol monomer is represented by four interaction sites centered on the carbons, oxygen, and the hydroxyl hydrogen. Interactions between sites in different monomers are described by the Coulomb and Lennard-Jones terms in eq 1. The three parameters for each site

$$\Delta E = \sum_{a}^{\text{in } A} \sum_{b}^{\text{in } B} \left(\frac{q_a q_b e^2}{r_{ab}} + \frac{A_a A_b}{r_{ab}^{12}} - \frac{C_a C_b}{r_{ab}^{6}} \right) \quad (1)$$

have been chosen to yield reasonable descriptions of liquid water and simple hydrocarbons and trends for series of dimers. The charges are also constrained to yield neutral monomers, so for ethanol $q(C_1) = -(q(O) + q(H_O))$ and $q(C_2) = 0$.

The geometry of the monomers is taken from standard values[4] and agrees closely with microwave data.[6] Specifically, r(OH), r(CO), and r(CC) are 0.945, 1.430, and 1.512 Å, and the COH and CCO angles are 108.5 and 107.8°. The lowest energy for the linear ethanol dimer with anti monomers is calculated by using the TIP function to be −5.99 kcal/mol at an OO separation of 2.805 Å.[4] In the simulations of methanol,[5] treating the alkyl hydrogens implicitly had little impact on the results for the liquid. By analogy the same simplification should be acceptable for ethanol.

The major conformational process in ethanol is the rotation about the CO bond. Microwave evidence supports the existence of both trans (ϕ = 180°) and gauche ($\phi \approx$ 60°) forms which is consistent with X-ray data for the solid.[7,8] However, the rotational potential surface including the trans–gauche energy difference has not been established experimentally.[22] Fortunately, ab initio molecular orbital calculations with moderate basis sets are generally reliable for such problems. Radom, Hehre, and Pople have

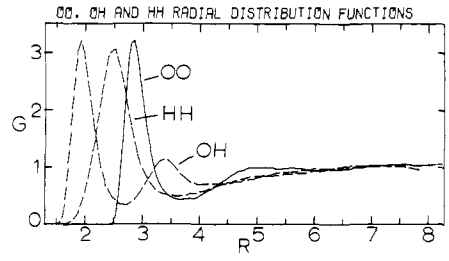

Figure 2. Computed OO, OH_O, and H_OH_O radial distribution functions for liquid ethanol at 25 °C. Interatomic distances are in Å throughout.

computed the rotational energy function for ethanol with the 4-31G basis set and fitted the results to the Fourier expansion given in eq 2.[9] Their $V(\phi)$ is plotted in the bottom half of Figure 1. The gauche–trans energy difference is 0.64 kcal/mol, and the intervening barrier is 1.35 kcal/mol. The highest point on the surface is for the cis conformation at 2.06 kcal/mol above trans. In view of the good agreement between 4-31G calculations and experimental barrier heights,[9] Pople's $V(\phi)$ has been used to describe the internal rotation in the Monte Carlo simulation of ethanol reported here.

$$V(\phi) = \tfrac{1}{2}V_1(1 - \cos\phi) + \tfrac{1}{2}V_2(1 - \cos 2\phi) + \tfrac{1}{2}V_3(1 - \cos 3\phi) \quad (2)$$

B. Monte Carlo Calculation. The Monte Carlo statistical mechanics simulation for liquid ethanol was executed with the TIP function in the usual manner.[4,5] Periodic boundary conditions and Metropolis sampling were employed for a cubic sample of 128 monomers (512 particles). The temperature was set at 25 °C, and the volume of the cube was determined by the experimental density, 0.785 09 g/cm^3.[10] Consequently, the length of an edge of the cube was 23.191 Å. The potential energy was obtained from the pairwise sum of the dimerization energies (eq 1) plus the internal rotational energy for the monomers (eq 2). A spherical cutoff at an OO separation of 9 Å was invoked in evaluating the dimerization energies. The significance of three-body effects in such calculations has been discussed and will receive additional attention below.[4,5,11,12]

New configurations were generated by randomly picking a monomer, translating it in all three Cartesian directions, rotating it about a randomly chosen axis, and finally performing the internal rotation about the CO bond. An acceptance rate for new configurations of 43% was obtained by using ranges of ±0.15 Å for the translations, ±15° for the complete molecular rotation, and ±15° for the internal rotation. The monomers were hydrogen bonded in the initial configuration, and their conformations were all cis (ϕ = 0°). The latter condition was chosen to help monitor the sampling efficiency. If the conformations were started from a Boltzman distribution or, for example, all trans and stayed that way, it would be more difficult to ascertain that ergodicity problems were not encountered. Since this is only the second Monte Carlo calculation to include an internal rotation,[5] the maximum height for barriers at a given temperature which still permits efficient sampling of configuration space has not yet been established. The low barrier of 2 kcal/mol used here is found to pose no difficulties at 25 °C.

The Monte Carlo run involved a total of 900K configurations. The first 500K were used to thoroughly equilibrate the system. The averaging for the reported results took place over only the final 400K configurations. The simulation was executed on the CDC/6600 system at Purdue University.

(5) Jorgensen, W. L., preceding paper in this issue.
(6) Harmony, M. D.; Laurie, V. W.; Kuczkowski, R. L.; Schwendeman, R. H.; Ramsay, D. A.; Lovas, F. J.; Lafferty, W. J.; Maki, A. G. *J. Phys. Chem. Ref. Data* **1979**, *8*, 619.
(7) Sasada, Y.; Takano, M.; Satoh, T. *J. Mol. Spectrosc.* **1971**, *38*, 33.
(8) Jönsson, P.-G. *Acta Crystallogr. Sect. B.* **1976**, *B32*, 232.
(9) Radom, L.; Hehre, W. J.; Pople, J. A. *J. Am. Chem. Soc.* **1972**, *94*, 2371
(10) Wilhoit, R. C.; Zwolinski, B. J. *J. Phys. Chem. Ref. Data, Suppl.* **1973**, *1*, 2.
(11) Jorgensen, W. L. *J. Am. Chem. Soc.* **1980**, *102*, 543.
(12) (a) Lie, G. C.; Clementi, E.; Yoshimine, M. *J. Chem. Phys.* **1976**, *64*, 2314. (b) Swaminathan, S.; Beveridge, D. L. *J. Am. Chem. Soc.* **1977**, *99*, 8392. (c) Jorgensen, W. L. *Ibid.* **1979**, *101*, 2011, 2016. (d) Jorgensen, W. L. *Chem. Phys. Lett.* **1980**, *70*, 326.

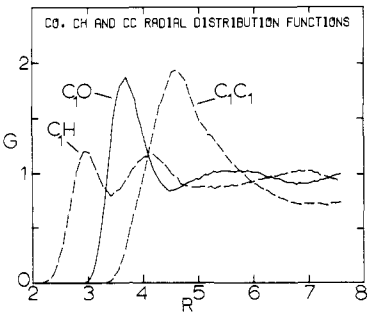

Figure 3. Computed C_1O, C_1H_0, and C_1C_1 radial distribution functions for liquid ethanol at 25 °C.

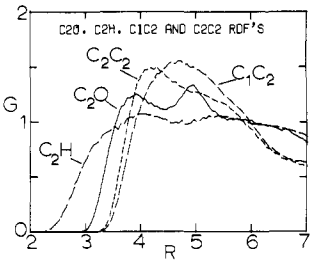

Figure 4. Computed C_2O, C_2H_0, C_1C_2, and C_2C_2 radial distribution functions for liquid ethanol at 25 °C.

III. Results and Discussion

A. Radial Distribution Functions. Radial distribution functions, $g_{xy}(r)$, represent fluctuations in the density of y atoms about atoms of type x due to local structure in the liquid. The density of y atoms is given explicitly by $\rho_{xy}(r) = \rho_y^\circ g_{xy}(r)$ where ρ_y° is the bulk density, N_y/V. The ten radial distribution functions (RDF's) corresponding to the different site–site interactions for the TIP model of ethanol are shown in Figures 2–4.

To assign the peaks, it is helful to refer to a chain model adopted from the solid as illustrated in I.[8] This is a much oversimplified

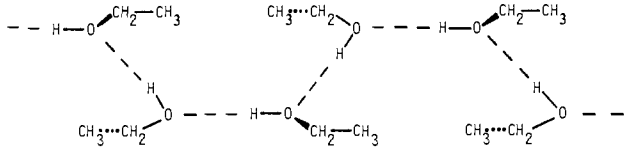

I

picture for the liquid as discussed below. It is noted that the chain structure is now U-shaped instead of V-shaped as in methanol (see I of the preceding paper). Also the monomers alternate gauche and trans. The structural differences in the solids appear to be influenced by an attempt to maximize the dispersion attraction between the ethyl groups in a 1,4-sense in ethanol and between methyls 1,3 in methanol. When the spectral and diffraction data for alcohols are analyzed, the V-shaped structure is often assumed as if it were the only possibility. This is clearly not the case.

Liquid ethanol has also been studied via X-ray diffraction by Harvey[13] and more recently by Wertz and Kruh.[14] They obtained the total atomic distribution curves, $\Gamma(r) = 4\pi r^2 \rho g(r)$, which include contributions from all pairs of nonhydrogen atoms. Thus, the peaks are not well resolved in comparison to Figures 2–4 and little structure is discernible beyond about 5 Å. Nevertheless, Wertz and Kruh assigned several peaks in $\Gamma(r)$ at 25 °C as reviewed in Table I by assuming the V-shaped chain structure. The calculated peak positions for the RDF's not involving hydrogen from the Monte Carlo run are listed for comparison.

The first peak in g_{OO} is due to the hydrogen-bonded neighbors and integrates to 1.9 from the TIP results which is close to the anticipated 2 (I). The peak occurs at 2.85 Å which is probably within the accuracy of the experimental estimate of 2.7 Å.[14]

(13) Harvey, G. G. *J. Chem. Phys.* **1939**, *7*, 878.
(14) Wertz, D. L.; Kruh, R. K. *J. Chem. Phys.* **1967**, *47*, 388.

Table I. Comparison of Calculated and Experimental Peak Positions in Radial Distribution Functions at 25 °C[a]

	TIP		X-ray[b]	
interactn	$g(r)$	$\Gamma(r)$	$\Gamma(r)$	assignt
OO	2.85	2.87	2.7	OO
OC_1	3.69	3.69	3.7	OC_1
OC_2	3.91	4.08	3.7	OO
C_2C_2	4.24	4.40	4.3	OC_2
C_1C_1	4.57	4.74	4.3	C_1C_1
C_1C_2	4.68	4.75	5.0	C_1C_2
OC_2	4.94	4.96	5.0	OC_2
OO	5.18	5.25	5.0	OO
OC_1	5.45			

[a] Peak positions in Å. [b] Data from ref 14.

Harvey reported 2.9 Å for this peak at −75 °C.[13] Furthermore, the OO separation in the solid at −186 °C is 2.72 Å.[8] The next peak in g_{OO} is calculated to occur at 5.18 Å, and there is an additional weak maximum at 7.6 Å. These features are readily assigned to the second and third nearest neighbors in the chains. The g_{OO} for methanol has three analogous peaks at somewhat shorter OO separation.[5] The sharper definition of the second and third peaks for methanol is consistent with the chain length averaging a little more than for ethanol (vide infra).

Wertz and Kruh erroneously assigned an OO contribution at 3.7 Å.[14] This is inconsistent with any reasonable chain model. Both theory and experiment find the first OC_1 peak at 3.7 Å which is due to nearest neighbors and has an analogue in methanol.[5] On the basis of Figure 4, the other contribution to the experimental peak near 3.7 Å is most likely from the first maximum in g_{OC_2} which Wertz and Kruh assigned at 4.3 Å. However, these authors neglected to assign any C_2C_2 peak. The later indeed has a computed maximum in Γ at 4.4 Å.

Most of the first peaks in the RDF's are for nearest-neighbor interactions; however, from I an exception may be $g_{C_2C_2}$ where the first peak could also involve some 1,4 contributions. Although most of the RDF's involving carbons show broad bands, the C_1H_0 and C_2O RDF's do reveal two maxima. For C_1H_0 this is reasonable in view of I since for a central monomer the C_1H_0 distance is shorter to the neighboring H-bond donor than to the neighboring acceptor. For C_2O, the two peaks probably have contributions from both gauche and trans methyls. If the central monomer is trans, then its methyl group is closer to the neighboring H-bond donor and about 1 Å farther from the neighboring acceptor. If it is gauche, then the methyl is closer to the acceptor and farther from the donor. In both cases, two peaks would result in g_{C_2O} as calculated.

The first peak in g_{OH} (Figure 2) corresponds to the hydrogen bonds. It integrates to 0.85 which implies roughly 1.7 hydrogen bonds per monomer. The first peak in g_{HH} integrates to 2.25, whereas 2 would be expected from Scheme I. One other point worth note is that the heights of the first peaks for the RDF's in Figure 2 have all increased noticeably from the values for the analogous peaks in methanol.[5] This is consistent with the deeper hydrogen-bonding well for ethanol; however, since the computed first peaks from pair potentials are generally too high, the effect is probably not desirable. Cooperative effects may be particularly important in this regard.

Before closing this section, one distribution related to g_{OO} should be discussed. It is for coordination numbers for neighbors within the range of the first peak in g_{OO}, 3.70 Å. Configurations were saved every 2000 attempted moves during the Monte Carlo run. Subsequently, when the OO distances within 3.70 Å in the saved configurations were analyzed, the neighbor distribution shown in Figure 5 was obtained. The inaccuracy of I for the liquid is apparent. Only about 55% of the monomers have two neighbors with the remainder having mostly one or three. These three environments correspond to monomers interior to chains or rings, chain ends, and Y junctions in the chains, respectively.

B. Stereoplots and Density. A particularly direct way to assess the structural features of a liquid is to display configurations of the periodic cube. The stereoplot in Figure 6 illustrates a typical

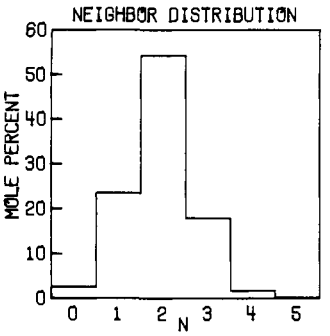

Figure 5. The distribution of coordination numbers for monomers defined by OO distances within the range of the first peak in g_{OO}, 3.70 Å.

configuration from the Monte Carlo simulation. Each of the 128 monomers is represented by four spheres, the methyl and methylene groups and the oxygen and hydrogen. It should be recalled that due to the periodicity monomers on one side of the cube are proximate to those on the opposite face. Also, the cube in the drawing is a bit outside the actual periodic cube which is more closely defined by the outermost oxygens.

A number of features should be noted from the stereoplot. (1) Hydrogen bonding is ubiquitous with most monomers participating in one or two H bonds. (2) Winding hydrogen bonded chains of various lengths are the dominant multimers. Two chains with at least five or six monomers are highlighted by the blackened oxygens. (3) The full range of conformations is represented with many monomers near gauche or trans. (4) In spite of the chains, there is great disorder in the liquid compared to the solid. There appears to be little correlation between the windings of nearby chains. (5) The occurrence of cyclic multimers is not obvious. This will be discussed further in the section on the H-bond analysis.

The pressure or density is usually not calculated in Monte Carlo calculations because it necessitates computing the intermolecular forces as well as the energy. Naturally, a slight error in the density leads to large discrepancies for the pressure. Furthermore, there is evidence that three-body interactions are essential to yield good computed pressures.[15] The even distribution of monomers in the stereoplot is consistent with the assigned density being reasonable or too high. If the potential function desired a higher density, sparsely populated regions would appear in the cube. The total density fluctuation, $\Delta\rho(R)$, defined in eq 3 has also been used as

$$\Delta\rho(R) = 1 + \int_0^R 4\pi\rho r^2 g(r)\, dr - 4/3\pi R^3\rho \qquad (3)$$

a diagnostic.[11] The function gives the difference in the number of neighbors calculated from an RDF and that expected by assuming uniform density in the cube. The results from g_{OO} in the simulation of ethanol are recorded in Figure 7. The oscillations are less than from experimental RDF's for water and ammonia.[16]

C. Thermodynamics and Internal Rotation. The thermodynamic results from the simulation are summarized in Table II and compared with the experimental heat of vaporization for the liquid going to the ideal gas, $\Delta H_V°$, and head capacity, C_V. E_i is the computed potential energy composed of the intermolecular term, E_i^{inter}, and the contribution from the internal rotation of the monomers, E_i^{rot}. As usual, E_i^{inter} includes a cutoff correction (−0.40 kcal/mol).[4] The $\Delta H_V°$ is computed from eq 4 and 5 as before.[5]

$$\Delta H_V° = \Delta E_V° + P(V°(g) - V(l)) \qquad (4)$$

$$\Delta E_V° \approx -E_i^{inter}(l) + E_i^{rot}(\text{ideal gas}) - E_i^{rot}(l) \qquad (5)$$

The energy of the internal rotation for the ideal gas was obtained from Pople's $V(\phi)$, eq 2, and the Boltzmann distribution. The computed $\Delta H_V°$ underestimates the experimental value by 16%. The difference can largely be attributed to the neglect of three-body effects in the simulation. Similarily, the C_V is also underestimated, though a longer Monte Carlo run might reduce the discrepancy since this property converges relatively slowly. The computed C_V includes the term for the variance of the intermolecular potential energy and a correction for the unimolecular contribution approximated by the heat capacity of the ideal gas at 25 °C, 13.7 kcal/mol.[4] Standard deviations (σ) were obtained from control functions for E_i (±0.02 kcal/mol), E_i^{rot} (±0.007 kcal/mol), and C_V^i (±0.9 kcal/mol).

Table II. Thermodynamic Properties for Liquid Ethanol at 25 °C[a]

	TIP	exptl
E_i^{inter}	−8.04	
E_i^{rot}	0.61	(0.61)[b]
E_i	−7.42	
$\Delta H_V°$	8.63	10.17[d]
C_V	20.4[c]	22.0[d,e]

[a] Energies in kcal/mol; heat capacities in cal/(mol deg). [b] Ideal gas result. [c] Includes ideal gas term. [d] Reference 10. [e] Computed from experimental C_P and coefficients of expansivity and compressibility.

The computed E_i^{rot} for the liquid is identical with the value for the ideal gas. The corresponding distributions, $S(\phi)$, for the dihedral angle are shown in the top half of Figure 1. The distributions for the full 360° range are given in Figure 8 which has been averaged due to the symmetry to yield Figure 1. The condensed phase is predicted to have little effect on the distribution of conformations. There is a slight increase in the gauche population; however, it is not enough to alter the energy. From integrating $S(\phi)$ between 120 and 240°, the trans population is 59.8% for the ideal gas and 57.7 ± 1.0% for the liquid. The corresponding gauche to trans ratios are 0.67 and 0.75 ± 0.03.[22]

It should be noted that the dipole moment for a monomer in the TIP model is invariant to ϕ since there is no charge on the methyl group. A large change in dipole moment is more apt to yield a phase dependence for $S(\phi)$. Experimentally, the gauche form of ethanol has been assigned a ca. 0.1 D greater dipole moment than the trans, though the difference is comparable to the error bars for the microwave measurements.[7] Similarly negligible effects have been computed recently for the conformational preferences of *n*-butane in going from the ideal gas to the liquid in molecular dynamics[17] and Monte Carlo[18] simulations. However, for liquid 1,2-dichloroethane (DCE) the dramatic increase in the gauche population observed experimentally is also predicted in a TIP-based Monte Carlo simulation.[18] A key difference between ethanol and DCE is the pattern of charges for the monomers. For DCE, a chlorine of one monomer can interact in a particularly constructive, unobstructed manner with *both* positively charged methylene groups of an adjacent monomer when it is gauche. In contrast, for ethanol since both groups adjacent to oxygen are positively charged and because the methyl group is roughly neutral, no significant gain is anticipated for having the hydrogen bond donor or acceptor either gauche or trans.

No sampling problems were evident for the internal rotation in the Monte Carlo calculation. The rotational energy converged readily and had a small standard deviation. In addition, Figure 8 witnesses that the conformational degree of freedom was thoroughly and nearly symmetrically sampled. Thus, a promising means for probing internal rotation in liquids has been discovered. Additional studies are planned to assess the limits of the procedure.

D. Energy Distributions. The distribution of bonding energies for monomers in liquid ethanol is shown in Figure 9. The curve is unimodal but not symmetrical. Similar distributions have been computed for other hydrogen-bonded liquids.[4,5,12b-d,16] The monomers experience a continuum of energetic environments covering a 20-kcal/mol range.

The distribution of dimerization energies for a monomer is displayed in Figure 10. The hydrogen-bonded neighbors are represented by the peak at low energy, and the distant bulk is in the spike near 0 kcal/mol. The shape is characteristic of hy-

(15) Barker, J. A.; Fisher, R. A.; Watts, R. O. *Mol. Phys.* **1971**, *21*, 657.
(16) Jorgensen, W. L.; Ibrahim, M. *J. Am. Chem. Soc.* **1980**, *102*, 3309.
(17) Weber, T. A. *J. Chem. Phys.* **1978**, *69*, 2347.
(18) Jorgensen, W. L.; Binning, R. C.; Bigot, B., submitted for publication.

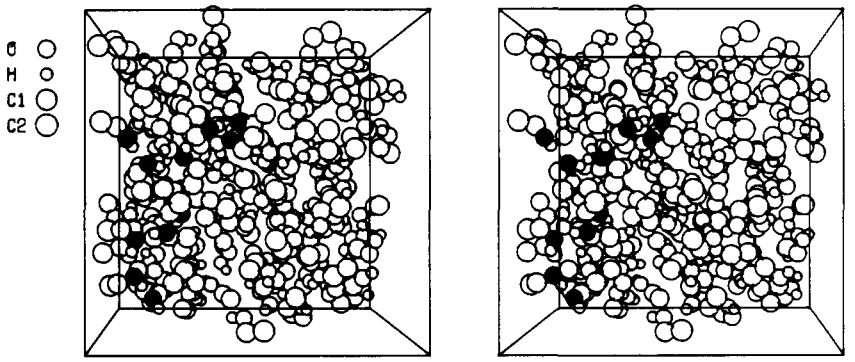

Figure 6. Stereoplot of a configuration from the Monte Carlo simulation of ethanol at 25 °C. Each of the 128 monomers is represented by four circles as indicated. The blackened oxygens point out two of the many hydrogen-bonded chains.

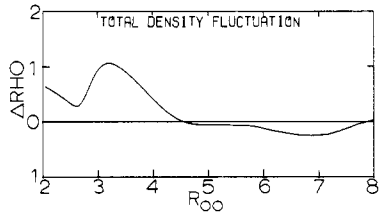

Figure 7. The total density fluctuation computed from the OO radial distribution function as defined in eq 3.

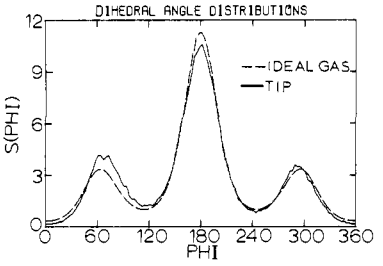

Figure 8. Complete population distributions for the CCOH dihedral angle, ϕ, from the Monte Carlo calculation for liquid ethanol and from a Boltzmann distribution for the ideal gas.

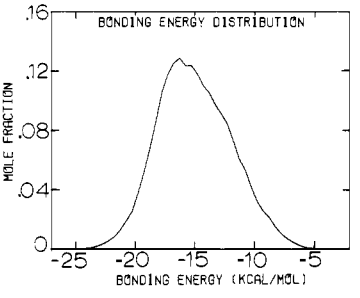

Figure 9. Computed distribution of intermolecular bonding energies for monomers in liquid ethanol. The units for the ordinate are mole fraction per kcal/mol.

drogen-bonded liquids.[4,5,12c-d,16] The minimum suggests an energetic limit of −2.25 kcal/mol for H bonding, which is the same figure as for methanol.[5] Integration to this point yields an average of 1.75 H bonds for each ethanol monomer in agreement with the estimate from the first peak in g_{OH}.

E. Hydrogen-Bonding Analysis and Infrared Data. The standard analyses of hydrogen bonding were made from the saved configurations by using the energetic definition of a hydrogen bond obtained from the energy pair distribution.[4,5,12d,16] The percentages of ethanol monomers in 0–4 hydrogen bonds are 4, 29, 56, 11, and 0%, as illustrated in Figure 11. From the ratio of monomers in one or two hydrogen bonds, an average chain length of 5–6 monomers can be estimated. All relevant data including the integrals of g_{OH} and the energy pair distributions from the TIP-based simulations indicate that the average chain length has diminished slightly in ethanol relative to methanol. The presence

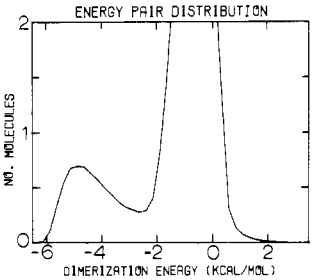

Figure 10. Computed distribution of dimerization energies for a monomer in liquid ethanol. The units for the ordinate are molecules per kcal/mol.

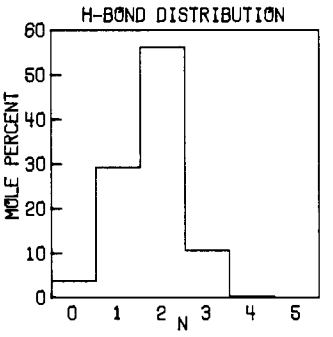

Figure 11. Computed distribution of hydrogen bonds in liquid ethanol. The percentage of monomers with N hydrogen bonds is given on the ordinate. A hydrogen bond is defined by a dimerization energy below −2.25 kcal/mol.

of small oligomers is also evident in the stereoplots, and the predicted occurrences of a small fraction of monomer and of chain branching are intriguing.

Association in alcohols has been carefully studied by infrared spectroscopy.[19] The experimental data indicate that H bonding does diminish as the alkyl groups are elaborated, and Luck estimates roughly 6% chain ends in liquid ethanol at 25 °C.[5,19] The beautiful matrix studies of Van Thiel, Hallam, and co-workers clearly establish the presence of small oligomers but predominantly multimers with more than four members in liquid methanol and ethanol.[19] Consistent with the solid, these higher multimers are found here to be chains. The occurrence of cyclic multimers in the stereoplots is very rare. In sharp contrast, Fletcher interpreted his IR data for ethanol-d_1 by using a model in which the liquid primarily consists of cyclic tetramers.[20] There is no doubt about the significant proportion of cyclic tetramers in the gas phase;[10,21]

(19) (a) Luck, W. A. P. In "The Hydrogen Bond", Schuster, P., Zundel, G., Sandorfy, C., Eds.: North-Holland Publishing Co: Amsterdam, 1976; Chapters 11, 28. (b) Hallam, H. E. *Ibid.*, Chapter 22. (c) Sandorfy, C. *Ibid.*, Chapter 13. (d) Luck, W. A. P.; Ditter, W. *Ber. Bunsenges. Phys. Chem.* **1968**, *72*, 365.

(20) Fletcher, A. N. *J. Phys. Chem.* **1972**, *76*, 2562.

(21) Coburn, W. C.; Grunwald, E. *J. Am. Chem. Soc.* **1958**, *80*, 1318.

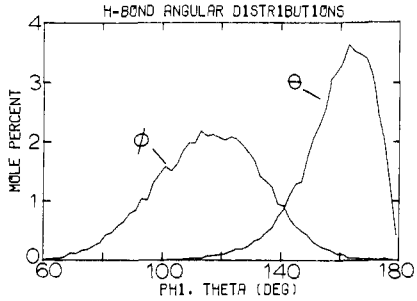

Figure 12. Computed distributions for the hydrogen-bonding angles, θ (0-H···0) and ϕ (H···O-H), between monomers with dimerization energies below -2.25 kcal/mol. The units for the ordinate are mole percent per degree.

however, the bulk of IR data rules out their dominance in the liquid.[19] The changes in thermodynamic properties of the lower alcohols are also most readily rationalized by increasing H bonding and average chain length as the temperature is lowered toward the freezing point. The prediction that there is branching of the chains corresponding to the 11% of monomers in three hydrogen bonds should be considered in future analyses of spectral results.

The distributions for the hydrogen bond angles, θ (0-H···O) and ϕ (H···O-H), from the Monte Carlo simulation are displayed in Figure 12. The results for methanol are nearly identical.[5] The average hydrogen bond is bent 15-20° and a wide variety of angular combinations is indicated. Thus, the picture that consistently emerges from liquid simulations is that hydrogen bonds are easily distorted and their geometries and energies are smoothly distributed over substantial ranges.[4,5,11,16] The distributions also eliminate the possibility of a significant fraction of small cyclic oligomers since they would be represented by values of θ near 60-120°. Of course, their population could be affected by the neglect of three-body effects.

IV. Conclusion

Simulations of liquid water, methanol, and ethanol have now been described by using the TIP model for the intermolecular interactions.[4,5] The results compare favorably with experimental thermodynamic and structural data and with the outcomes of simulations using other potential functions. No severe discrepancies with experiment have been found, though the computed flatness of g_{OO} beyond the first peak for water was disappointing. The combined simplicity, transferability, and utility of the TIP functions is certainly impressive in view of the difficulties that have previously been encountered in generating useful intermolecular potential function. The approach and TIP parameters will be extended and may require some revisions.

As shown here, the results of liquid simulations can be most valuable in interpreting experimental diffraction and spectroscopic data. The potential for studying conformational problems in the liquid phase via Monte Carlo calculations has also been established. Thus, important strides have been made toward opening up organic chemistry in solution to theoretical investigation at the molecular level.

Acknowledgment. Gratitude is expressed to the National Science Foundation for financial assistance. Acknowledgement is also made to the donors of the Petroleum Research Fund, administered by the American Chemical Society, for support of this research. The work was facilitated by the National Resource for Computation in Chemistry under a grant from the National Science Foundation (Grant CHE-7721305) and the Basic Energy Sciences Division of the U.S. Department of Energy (Contract No. W-7405-ENG-48). Mr. P. Cheeseman kindly provided the program to create the stereoplots.

(22) **Note Added in Proof**: A recent microwave study of ethanol yielded a trans-gauche energy difference of 0.12 ± 0.01 kcal/mol which is significantly lower than the ab initio value of 0.64 kcal/mol.[23] Thus, the actual trans populations in the gas and liquid may be ca. 20% lower at 25 °C than computed here.

(23) Kakar, R. K.; Quade, C. R. *J. Chem. Phys.* **1980**, *72*, 4300.

Synthesis and Structure of Carborane-Substituted Cyclic and Polymeric Phosphazenes

H. R. Allcock,* A. G. Scopelianos, J. P. O'Brien, and M. Y. Bernheim

Contribution from the Department of Chemistry, The Pennsylvania State University, University Park, Pennsylvania 16802. *Received June 11, 1980*

Abstract: The synthesis of the first carborane-substituted cyclophosphazenes together with the preparation, by two different approaches, of the first carborane-substituted phosphazene linear polymers is reported. The cyclic derivatives IV are both precursors and model compounds for the analogous polymeric derivatives VI. The crystal and molecular structure of IV (R = phenyl) has been investigated by single-crystal X-ray diffraction techniques. The molecule contains a planar phosphazene trimer ring bound directly to the phenyl carboranyl group through a P-C bond. The absence of steric and electronic influences by the phosphazene and carboranyl units on each other is discussed. The crystals of IV (R = phenyl) are monoclinic with the space group $P2_1/n$ and with a = 9.476 (3) Å, b = 12.984 (2) Å, c = 18.726 (3) Å, and β = 100.11 (3)° with V = 2268.2 (3) Å^3 and Z = 4. The P-N bond distances are all similar and average 1.574 Å. The P-C bond length is 1.820 Å, and the Cl-P-C angle was found to be 102.4°. The reaction between high molecular weight poly(dichlorophosphazene), $(NPCl_2)_n$, and methyl- or phenyl-1-lithio-*o*-carborane was also studied. Chlorine substitution is a slow process, and is accompanied by chain cleavage. The nucleophilic replacement of the halogen atoms yielded high polymers of structure IX that contain up to 15% of the side groups as carboranyl units. The remaining chlorine atoms were replaced by treatment with sodium trifluoroethoxide. The properties and structure of the macromolecules are discussed.

In recent years wide ranging synthetic advances have taken place in two separate areas of main group inorganic chemistry—in phosphazene chemistry on the one hand and in the chemistry of polyhedral boranes and carboranes[1,2] on the other. In this paper we make a connection between these two fields and explore the influence of a linked carborane cage on a phosphazene ring and on a phosphazene high polymeric chain.

Modern phosphazene chemistry is dominated by nucleophilic substitution reactions that involve the use of halophosphazene cyclic trimers or high polymers (I or II) as substrates for reactions with alkoxides, aryloxides, or amines (Scheme I).[3-7] To a more

(1) Grimes, R. N. "Carboranes"; Academic Press: New York, 1970.
(2) Hawthorne, M. F. *J. Organomet. Chem.* **1975**, *110*, 97.

0002-7863/81/1503-350$01.00/0